

COPLANAR WAVEGUIDE VS. MICROSTRIP  
FOR MILLIMETER WAVE INTEGRATED CIRCUITS

R.W. Jackson

Department of Electrical and Computer Engineering  
University of Massachusetts  
Amherst, MA 01003

## ABSTRACT

Using a full wave analysis, coplanar waveguide transmission line is compared to microstrip in terms of conductor loss, dispersion and radiation into parasitic modes. It is shown that, on standard .1 mm semiconductor at 60 GHz, the dimensions of coplanar waveguide can be chosen to give better results in terms of conductor loss and dispersion than microstrip. Curves are presented comparing the microstrip open end and the coplanar waveguide short circuit in terms of parasitic mode generation.

## INTRODUCTION

For many years monolithic microwave integrated circuits have predominately used microstrip transmission lines. At microwave frequencies microstrip is well understood and flexible in that a large number of circuit elements can be made with it. However, for integrated circuits operating at millimeter wave frequencies it may not be the medium of choice. One disadvantage is that via holes are required to ground active devices. At millimeter wave frequencies these vias can introduce significant inductance and degrade circuit performance.

Coplanar waveguide has been suggested as an alternate to microstrip [1] but has not been widely used due to the mistaken assumption that it has inherently higher conduction loss than microstrip. Its principle advantage is that it is well suited for use with field effect transistors, especially at millimeter wave frequencies where R.F. grounding must be close to the device. Via holes are not necessary and fragile semiconductors need not be made excessively thin.

This paper compares coplanar waveguide to microstrip in terms of conductor and dielectric loss, dispersion characteristics and radiation of parasitic modes. A full wave technique is used to determine the currents in the vicinity of infinite lines on open substrate. These currents are then used to calculate loss [2] and impedance. Radiation at the aforementioned discontinuities is also determined using a full wave analysis [3] which is described briefly. A standard .1 millimeter thick GaAs substrate is assumed throughout as well as a 60 GHz operating frequency. The conclusions with regard to the comparison are not particularly sensitive to this choice of frequency.

## INFINITE LINE ANALYSIS

Full wave analysis techniques are well known for infinite transmission lines [4], [5]. The techniques presented in this section outline the methods used for calculation of the loss, impedance and dispersion in coplanar waveguide (CPW). The same techniques were used to obtain the same quantities in microstrip.

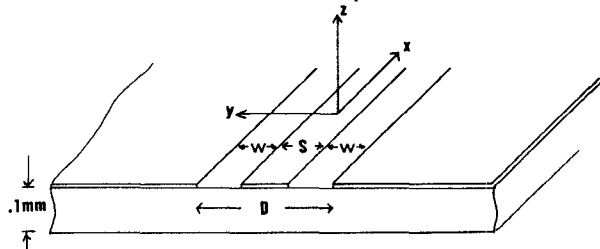


Figure 1. Structure of the coplanar waveguide transmission line.

For coplanar waveguide, currents on the  $z=0$  plane (see Figure 1) are determined by the slot fields according to the relation

$$\begin{bmatrix} J_y(y) \\ J_x(y) \end{bmatrix} = \int_{-\infty}^{\infty} dk_y \begin{bmatrix} \tilde{g}_{yy} & \tilde{g}_{xx} \\ \tilde{g}_{xy} & \tilde{g}_{xx} \end{bmatrix} \cdot \begin{bmatrix} \tilde{E}_y(k_y) \\ \tilde{E}_x(k_y) \end{bmatrix} \exp(jk_y y) \quad (1)$$

where an  $\exp(-jk_y x)$  dependence has been suppressed. The  $\tilde{g}_{ij}$  (see appendix) are the Fourier transform of the Green's function and are dependent upon  $\beta$  and  $k_y$ . Following references [4] and [5] we expand  $E_y(y)$  in terms of the functions shown below.

$$\begin{aligned} E_y(y) &= \sum_{n=0}^{\infty} A_n \frac{\cos(n\pi[u/w+1/2])}{\sqrt{1-(2u/w)^2}}, \\ E_x(y) &= \sum_{n=0}^{\infty} B_n \frac{\sin(n\pi[u/w+1/2])}{\sqrt{1-(2u/w)^2}}, \\ u &= |y| - (S+w)/2, \quad -w/2 < u < w/2 \end{aligned} \quad (2)$$

The constants  $\beta$ ,  $A_n$  and  $B_n$  are determined such that weighted moments of  $J_y$  and  $J_x$  in the slot are zero. The chosen weighting functions are the same as the

expansion functions. As usual  $\beta$  is varied until nontrivial values of  $A_n$  and  $B_n$  can exist. The  $A_n$  and  $B_n$  can then be used with (1) and (2) to determine  $J_x^n$  and  $J_y^n$  everywhere on the conductors.

Characteristic impedance is defined using a voltage-current definition,

$$Z_c = V \cdot \left[ 2 \int_0^s dy J_x(y) \right]^{-1}$$

where  $V$  is the voltage across the gap. This definition is not the only one possible, but it is felt that it reflects the character of the local fields more accurately than the power-voltage definition and the local fields are most significant to circuit modelers. Microstrip impedances are also defined using a voltage-current model where the current is the  $x$ -directed current on the strip and the voltage is the line integral of the  $E_z$  field under the strip average over the strip width.

Conductor loss is determined from the formula

$$\alpha = C \frac{Z_c}{V^2} \left[ \int_0^{S/2-\Delta} dy + \int_{S/2+w+\Delta}^{\infty} dy \right] \cdot \left[ |J_y^u|^2 + |J_x^u|^2 + |J_y^l|^2 + |J_x^l|^2 \right] \quad (4)$$

where  $\Delta = t/290$ ,  $t$  is the conductor thickness, and  $C$  is a constant which includes surface resistivity. The choice of  $\Delta$  is made according to Lewin's work [2] in order to avoid the nonintegrable singularity at the edge of the zero thickness conductor assumed in the full wave analysis. The  $u$  and  $l$  superscript on the current refer to the current on the upper and lower sides of the conductor. These currents were calculated using equation 1 with different Green's functions (see appendix). The  $y$  integration in (4) and the  $k_y$  integration in (1) were performed numerically. When computing currents near the conductor edges the integration in (1) is very slow to converge and one must subtract the asymptotic value of the integrand and evaluate it analytically.

Dielectric loss is calculated using standard formulas and is only a small part of the total loss.

#### INFINITE LINE COMPARISON

Figure 2 shows conductor and dielectric loss plotted against impedance for microstrip and coplanar waveguide on a substrate with a permittivity of 12.8. A conductor thickness of 3 microns is chosen. Copper conductor was assumed, but any other conductor would result in the same conclusions as far as comparisons are concerned. The coplanar waveguide impedance is varied by keeping a constant cross-section ( $D$ ) and changing the center conductor width. For microstrip the only free parameter is the strip width. Strip widths were constrained to be between 10 and approximately 300 microns.

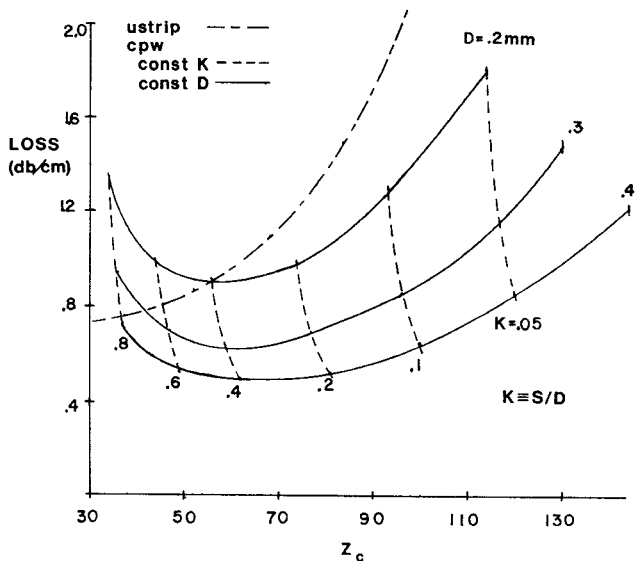


Figure 2. Comparison of microstrip and coplanar waveguide losses for  $\epsilon_r = 12.8$ ,  $f = 60$  GHz, .1 mm substrate thickness, substrate loss tangent of .0006 and a 3 micron conductor thickness.

The figure shows that coplanar waveguide can have significantly less loss than microstrip over a broad range of impedances but especially at higher impedances. The impedance for minimum coplanar waveguide loss appears to be about 60 ohms for any of the chosen cross-sections. The microstrip width at minimum loss is about 300 microns whereas the smallest coplanar waveguide cross-section which will give the same loss is about 250 microns. So sizes are comparable.

The loss calculation shows the size that coplanar waveguide must be in order to compete with microstrip. For these sizes figure 3 shows a comparison of dispersion for microstrip and coplanar waveguide. The fractional change in effective dielectric constant per fractional change in frequency is plotted against impedance. For frequencies near 60GHz the figure shows that coplanar waveguides with cross-sections between 200 and 300 microns have as much or less dispersion than microstrip.

#### ANALYSIS OF PARASITIC RADIATION LOSS

One way of comparing microstrip and coplanar waveguide in terms of parasitic radiation is to compare radiation (surface wave and space wave) from a coplanar waveguide short circuit and from a microstrip open circuit using the dimensions given in section 1.

The analysis of losses from a microstrip open end and coplanar waveguide short circuit has been reported previously [3]. In that work the authors used a moment method technique to calculate the slot fields (strip currents) at the end of a coplanar waveguide (microstrip). These fields (currents) were assumed to be transverse (longitudinal). The analysis which is presented

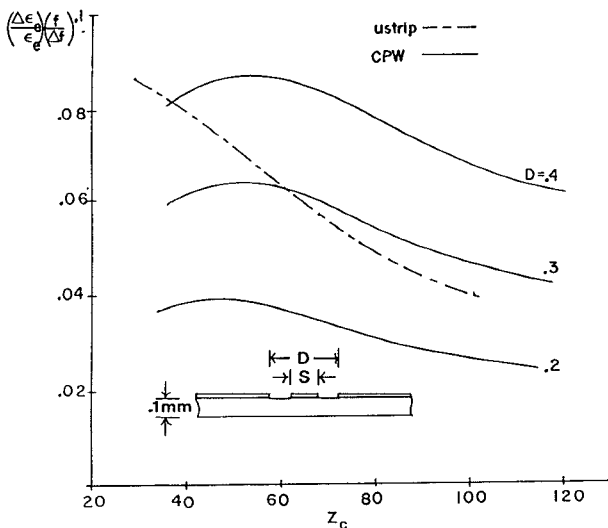


Figure 3. Comparison of microstrip and coplanar waveguide dispersion.

here also includes the longitudinal fields (transverse currents). In the previous analysis of the coplanar waveguide short, the slot fields were assumed to be symmetric around the slot centers. For tightly coupled slots, this can be inaccurate as Jansen [4] points out. The possible asymmetry is allowed in the analysis which is now outlined. Only the differences between this calculation and the calculations in reference 3 will be discussed.

The coordinate system used is shown in Figure 1 except that the slots only exist  $x < 0$ . Slot fields are related to  $z=0$  surface currents by an equation similar to (1) except that  $J$  is a function of  $x$  and  $y$ ,  $g_{ij}(\beta, k_y)$  is replaced by  $G_{ij}(k_x, k_y)$ ,  $E$  is a function of  $k_y$  and  $k_x$  and the inverse Fourier transform is with respect to both  $k_x$  and  $k_y$ . The slot fields are expanded in terms of known functions multiplied by unknown constants,

$$E_\alpha(x, y) = g^\alpha(y) [(1+R)f_c(x) + j(1-R)f_s(x) + \sum_{n=1}^N A_n^\alpha f(x-x_n)], \quad \alpha = x \text{ or } y. \quad (5)$$

The functions  $f_c$  and  $f_s$  are cosine and sine functions which are several periods in length,  $f(x)$  is a piecewise sinusoidal function,  $R$ , the reflection coefficient, and  $A_n^\alpha$  are unknown constants. For the coplanar waveguide the transverse dependence of the fields  $g^y(y)$  and  $g^x(y)$  is made up of three pulse and three triangle functions, respectively (see figure 4). The amplitudes of all six functions are related to each other and are computed prior to the discontinuity calculation. This relationship as well as the propagation constant used in  $f$  was obtained by using pulse and triangle functions as expansion modes in the infinite line solution which was described in the first section of this paper. Due to the similarity of the expansion functions to one another, the amplitudes and propagation constant can be calculated very quickly. The propagation constants so calculated are within 1% of those calculated using modes in equation 2 for all impedances of interest. By using this type of

function for  $g^\alpha(y)$ , the asymmetry in the slot fields can be included in the analysis of the short circuit discontinuity.

Weighting functions are chosen to be the piecewise sinusoidal parts of equation 5,  $f(x-x_n)g^y(y)$  for  $x$ -directed fields and  $f(x-x_n)g^x(y)$  for  $y$ -directed fields. All piecewise modes were located in the range  $0 > x > -\lambda_g/4$ . Sufficient expansion modes were used such that the end resistance and length extension converge to within an estimated 5% of their final value. Although length extension was not a goal of this calculation, this method

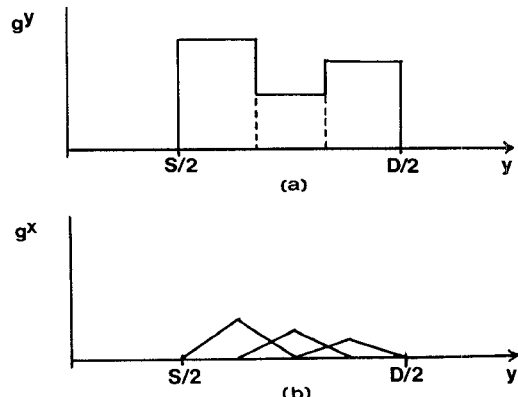


Figure 4. Transverse variation of slot fields, for  $y > 0$ , (a)  $E_y$  and (b)  $E_x$ .

produced results which were within 10% of those calculated by Jansen [4].

Loss from an open ended microstrip was calculated in a similar manner except that the transverse variation of the  $x$  and  $y$  directed strip currents were, respectively,

$$\frac{1}{\sqrt{1-(2y/w)^2}} \text{ and } \frac{\sin(\pi[y/w+1/2])}{\sqrt{1-(2y/w)^2}}.$$

#### COMPARISON OF DISCONTINUITY LOSS

Figure 5 compares power lost due to space wave and surface wave radiation from a microstrip open end and a coplanar waveguide short circuit. These values are obtained from end impedance calculations by the relationship

$$\frac{P_{\text{rad}}}{4P_{\text{incidence}}} = \begin{cases} GZ_c, \text{ open end microstrip} \\ RY_c, \text{ short circuit CPW} \end{cases}$$

where  $G$  ( $R$ ) is the real part of the end admittance (impedance). Coplanar waveguide size ( $D$ ) is chosen in accordance with the conductor loss results in the second section. The coplanar waveguide evidently radiates much less energy.

#### CONCLUSIONS

It has been shown that, at millimeter wave frequencies, coplanar waveguide can be equal to or better than microstrip when loss and dispersion on GaAs substrate are used as a basis for comparison. Minimum loss for a given coplanar waveguide cross-section occurs at about a 60 ohm impedance whereas the minimum loss for microstrip occurs at about 25

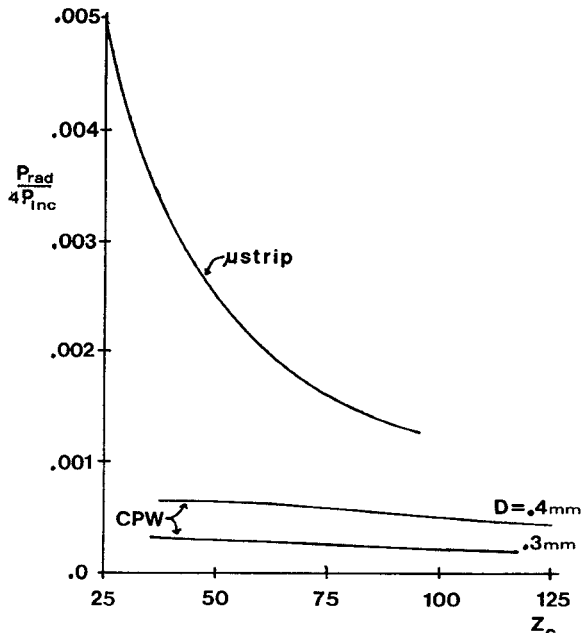


Figure 5. Comparison of microstrip and coplanar waveguide discontinuity loss.

ohms. The physical sizes at these minimum loss impedances are similar. This is important when long runs of transmission line are being contemplated. For higher impedances coplanar waveguide can give much smaller loss but will take up more space than the same impedance microstrip line.

Using the coplanar waveguide sizes required to make conductor loss comparable to that of microstrip, we have calculated discontinuity radiation loss for the two types of lines. A full wave analysis which includes space wave and surface wave radiation shows that coplanar waveguide discontinuities radiate much less energy than microstrip discontinuities.

The disadvantages of coplanar waveguide compared to microstrip are; size, the possibility that an even mode can be excited at non symmetric discontinuities and possibly heat transfer for active devices.

The advantages of coplanar waveguide include; easier construction using thicker substrates and no via holes, good grounding for integrated active devices, less radiation at discontinuities and, in some cases, lower conductor loss.

#### ACKNOWLEDGEMENT

This work was supported by the General Electric Company and by the Airforce Office of Scientific Research under contract #F49620-82-C-0035.

#### APPENDIX

The following functions are the Fourier transform of the Green's function which relates an infinitesimal slot electric field (magnetic current) at  $x=y=z=0$  to the electric current on the lower side of a conductor on the  $z=0$  plane.

$$\tilde{G}'_{xy}(k_x, k_y, \epsilon_r) = \frac{-1}{\omega \mu} \frac{k_x^2 k_1 (1 - \epsilon_r)}{TM \cdot TE} + \frac{k_x k_y (k_1 \cos k_1 d + j \epsilon_r \sin k_1 d)}{k_1 TM},$$

$$\tilde{G}'_{xy}(k_x, k_y, \epsilon_r) = \frac{-1}{\omega \mu} \frac{k_x k_y k_1 (1 - \epsilon_r)}{TM \cdot TE} + \frac{k_x k_y (k_1 \cos k_1 d + j \epsilon_r k_2 \sin k_1 d)}{k_1 TM},$$

$$TE = k_1 \cos k_1 d + j k_2 \sin k_1 d, \quad TM = \epsilon_r k_2 \cos k_1 d + j k_1 \sin k_1 d$$

$$k_2 = k_o^2 - \beta^2, \quad k_1 = \epsilon_r k_o^2 - \beta^2, \quad \beta^2 = k_x^2 + k_y^2$$

Except for loss calculations, only the total current from both the lower and upper sides is of interest,

$$\tilde{G}_{yy}(k_x, k_y) = \tilde{G}'_{yy}(k_x, k_y, \epsilon_r) + \tilde{G}'_{yy}(k_x, k_y, 1),$$

$$\tilde{G}_{xy}(k_x, k_y) = \tilde{G}'_{xy}(k_x, k_y, \epsilon_r) + \tilde{G}'_{xy}(k_x, k_y, 1),$$

$$\tilde{G}_{yx} = \tilde{G}_{xy}, \quad \tilde{G}_{xx}(k_x, k_y) = \tilde{G}_{yy}(k_x, k_y, k_x).$$

For an infinite line the  $x$  variation is determined by the propagation constant,  $\beta$ , and therefore the Green's functions used in equation 1 are,

$$\tilde{g}_{yy}(\beta, k_y) = \tilde{G}_{yy}(\beta, k_y), \quad g_{yx}(\beta, k_y) = \tilde{G}_{xy}(\beta, k_y),$$

$$\tilde{g}_{xy}(\beta, k_y) = \tilde{G}_{xy}(\beta, k_y), \quad \tilde{g}_{xx}(\beta, k_y) = \tilde{G}_{yy}(k_y, \beta).$$

#### REFERENCES

- [1] R. A. Pucel, "Design Considerations for Monolithic Microwave Circuits", IEEE Trans. MTT-29, pp. 513-534, April 1981.
- [2] L. Lewin, "A Method of Avoiding the Edge Current Divergence in Perturbation Loss Calculations", IEEE Microwave Theory and Tech., MTT-32, No. 7, pp. 717-719, July 1984.
- [3] R. W. Jackson and D. M. Pozar, "Surface Wave Losses at Discontinuities in Millimeter Wave Integrated Transmission Lines", IEEE Microwave Symposium Digest, MTT-S, pp. 563-565, June 1985.
- [4] R. Jansen, "Unified User-oriented Computation of Shielded, Covered and Open Planar Microwave and Millimeter-wave Transmission-line Characteristics", Microwave, Optics and Acoustics, Vol. 3, No. 1, pp. 14-22, January 1979.
- [5] T. Itoh, "Spectral-domain Inmittance Approach for Dispersion Characteristics of Generalized Printed Transmission Lines", IEEE Trans. Microwave Theory Tech., Vol. MTT-28, p. 733-736, July 1980.
- [6] R. Jansen, "Hybrid Mode Analysis of End Effects of Planar Microwave and Millimeter Transmission Lines", IEEE Proc., Vol. 128, PT.H, No. 2, pp. 77-86, 1981.